Electronic Supplementary Material (ESI) for Chemical Communications.

Supporting Information

A novel photoswitchable enzyme cascade for powerful signal amplification in versatile bioassays

Guang-Li Wang*, Xiao-Qin Li, Gen-Xia Cao, Fang Yuan, Yuming Dong, Zaijun Li

*The Key Laboratory of Synthetic Colloids and Biotechnology, Ministry of Education, School of Chemical and Material Engineering, Jiangnan University, Wuxi 214122, Jiangsu, China.
*Fax: +86-510-85917763. E-mail: glwang@jiangnan.edu.cn.

Experimental section

Reagents

L-Dihydroxyphenylalanine (DOPA), tyrosinase (TYR), and horseradish peroxidase (HRP) were purchased from Aladdin Industrial Corporation (Shanghai, China). Tyrosine was purchased from Hushi Laboratorial Equipment Co., Ltd. (Shanghai, China). Superoxide dismutase (SOD) from bovine liver, catalase (CAT), glucose oxidase (GOx) and apurinic/apyrimidinic endonuclease (APE-1) and apurinic/apyrimidinic endonuclease antibody (anti-APE-1, monoclonal antibody) were purchased from Sigma-Aldrich (St. Louis, USA). Alkaline phosphate (ALP) and thrombin (TB) were purchased from Shanghai Yuanye Biological Technology Co., Ltd. (Shanghai, China). Titanium tetrachloride ($TiCl_4$), t–butanol (TBA), isopropanol (IPA), ethylene diamine tetraacetic acid (EDTA), potassium iodide (KI), 3,3',5,5'-tetramethylbenzidine (TMB), glycine (Gly), threonine (Thr) and bovine serum albumin (BSA) were all obtained from Sinopharm Chemical Reagent Co., Ltd. (Shanghai, China). Alpha fetoprotein (AFP), carcinoembryonic antigen (CEA), interleukin-6 (IL-6) were purchased from Jorferin Bio-Technology Co., Ltd. (Beijing, China). Rabbit IgG was purchased from Shfeng Biological Technology Co., Ltd. (Shanghai, China). Goat IgG obtained from Boster Biological Technology, Co., Ltd. (Wuhan, China).

For conducting the immunoassay, the washing buffer solution was 0.01 mol/L phosphate buffer saline (PBS) (pH 7.4) containing 0.05% Tween 20. The blocking buffer solution was 0.01 mol/L PBS (pH 7.4) containing 3% (w/v) BSA.

Apparatus

High resolution transmission electron microscopy (HRTEM) images were performed using a JEOL JEM–2100 transmission electron microscope (Hitachi, Japan). Scanning electron microscopy (SEM) images were captured on a Hitachi S-4800 high resolution scanning electron microscope (Hitachi, Japan). The crystal structures of TiO_2 samples were characterized by X–ray powder diffraction (XRD), obtained using an X'Pert Philips materials research diffractometer using Cu K_α radiation and employing a scanning speed of 0.04° s^{-1} in the 2θ range of 20 to 75°. Fourier transform infrared (FT−IR) spectrum was recorded on a Nicolet FT−IR 6700 spectrometer (ThermoFisher, USA) using the KBr method. UV–vis absorption spectroscopic measurements were carried out using a TU–1901 spectrophotometer (Beijing Purkinje General Instrument Co., Ltd., China). A 300 W Xe lamp (NBeT, China) equipped with an ultraviolet cutoff filter ($\lambda \geq 400$ nm) was used as the irradiation source. The detection of TYR by the absorption method was conducted on 96 well plates by an enzyme labeled meter (SpectraMax M5, USA). Photoelectrochemistry and linear potential scans were conducted on a CHI 800C electrochemical workstation in 0.1 mol/L Na_2SO_4 aqueous solution

using a three-electrode system: TiO_2 or TiO_2/DOPA modified indium tin oxide (ITO) electrode was served as the working electrode, a Pt wire was used as the counter electrode, and a saturated Ag/AgCl as the reference electrode.

Hydrothermal synthesis of TiO_2 NPs

TiO_2 NPs were synthesized according to a modified procedure[1].Typically, 1.0 mL of $TiCl_4$ was slowly added to 10 mL distilled water at room temperature. The hydrolysis reaction was highly exothermic and produced high quantities of fumes of HCl. After about 10 h of continuous stirring, a white solution was formed and then it was boiled for another 2 h to eliminate most of the chloride ions as HCl gas, which produced milky white TiO_2 suspensions. The acquired products were filtered and washed with distilled water several times and dried at 333 K for 12 h to produce white TiO_2 nanopowders. A 1.0 mg/mL of TiO_2 suspension was prepared by redispersing the as-prepared TiO_2 NPs in water through ultrasonication.

Investigation of the catalytic characteristics of TiO_2/DOPA and TiO_2/DOPA-HRP for the oxidation of TMB under visible light (λ≥400 nm) irradiation

The TiO_2/DOPA were acquired by mixing L-DOPA (1.0×10^{-4} M) with the 1.0 mg/mL TiO_2 NPs' solution and stirred for a moment at room temperature followed by centrifugation and redispersion in 1.0 mL of ultrapure water. For the catalyzed oxidation of TMB using illuminated TiO_2/DOPA or TiO_2/DOPA−HRP, specifically, 0.01 mg/mL of TiO_2/DOPA in the absence or presence of 10 mg/mL HRP in a reaction volume of 1.0 mL acetate buffer solution (40 mM, pH 4.0) with 500 μM TMB as the substrate were irradiated with a 300 W Xe lamp equipped with an ultraviolet cutoff filter (λ≥400 nm) to provide visible light. The absorbance of the oxidized product (oxTMB) was recorded at 652 nm.

The reaction kinetics for the catalytic oxidation of TMB by the TiO_2/DOPA−HRP was studied by monitoring the absorption intensity of the oxTMB at 652 nm with a 1 min interval. Catalytic experiments were carried out at 40 ºC using 0.01 mg/mL of TiO_2/DOPA and 10 mg/mL HRP in 1.0 mL acetate buffer solution (40 mM, pH 4.0) with varied concentrations of TMB under visible light irradiation.

Probing the activity of TYR through the photoswitchable enzyme cascade

The TYR activity assay was conducted in a 96 well plate based on its enzymatically catalytic oxidation of L-tyrosine to generate L-DOPA for conjugating with TiO_2 NPs to form TiO_2/DOPA for activating HRP. Specifically, 0.15 mg/mL TiO_2 and 10 μL TYR with different concentrations were mixed with 10 μL of 0.01 M L-tyrosine for an incubation time of 10 min with gentle shaking in 50 μL of acetate buffer (pH=7.0) solution at 37 ºC in the 96 well plates. Subsequently, 160 μL of acetate buffer solution (pH=4.0), 20 μL of 100 mg/mL HRP and 20 μL of 5.0 mM TMB were added in the above solution and then illuminated for 15

min at 40 ºC under visible-light (λ≥400 nm). Finally, the absorbance of the oxTMB at 652 nm was measured by an enzyme labeled meter.

Immunoassay of APE-1 based on the photoswitchable enzyme cascade

Preparation of the TYR/Au NPs/Ab_2 bioconjugates. Firstly, Au NPs were prepared by referring to the literature[2]. That is, 2.5 mL of 1% trisodium citrate solution was quickly added to the boiled $HAuCl_4$ solution (100 mL 0.01%) under vigorous stirring and the solution turned to be deep red, indicating the formation of Au NPs. Followed by continued stirring for 12 h and cooling down, Au NPs were prepared. Subsequently, 1.0 mL of the obtained Au NPs solution was adjusted to pH 8.5 with (0.1 mol/L) Na_2CO_3 followed by the addition of 20 μL of the detection antibody (Ab_2, 0.4 mg/mL) and TYR (40 μL, 0.4 mg/mL). The above mixture was then stirred for 12 h at 4 ºC, followed by treating with 0.1% BSA to block non-specific adsorption. After that, the mixture was centrifuged at 15,000 g for 15 min. The precipitated TYR/Au NPs/Ab_2 bioconjugates were resuspended in 1.0 mL of PBS (pH=7.4) buffer and stored at 4 ºC for use.

The sucessful synthesis of the TYR/Au NPs/Ab_2 bioconjugates was verified by the UV-Vis absorption spectroscopy (as show in Fig.S9, in ESI†). The absorption peak at 274, 278 and 523 nm (curve a, b and c) were assigned to TYR, Ab_2 and Au NPs respectively. Compared with the absorption spectrum of the individual component, the TYR/Au NPs/Ab_2 bioconjugates' spectrum contains two characteristic peaks at 277 and 533 nm, corresponding to the absorption of TYR/Ab_2 and Au NPs, respectively. This demonstrated that TYR/Au NPs/Ab_2 bioconjugates were successfully obtained. The absorption peak of Au NPs red shifted slightly in the TYR/Au NPs/Ab_2 bioconjugates, which might be due to the Au-S interaction between Au NPs and thiolated protein, which will change the Au NPs' size and their aggregation state, thus leading to variation in the surface plasmon resonance properties of the Au NPs.

A sandwich immunoassay conducted on the 96 well plates was used for the detection of APE-1. A 20 μL of 0.1 mg/mL monoclonal antibody (anti-APE-1, capture antibody, Ab_1) was firstly spread onto the 96 well plates and incubated at 4 ºC overnight followed by washing to remove the excess Ab_1. The wells were then blocked with 20 μL of the blocking solution for 2 h at 4 ºC to block nonspecific binding sites and washed with the washing buffer thoroughly. Next, 20 μL of AEP-1 with different concentrations were dropped onto the Ab_1 modified wells for an incubation time of 60 min at 37 ºC followed by washing. After the immunoreaction between Ab_1 and the APE-1, the wells were allowed for labeling by an additional incubation with 20 μL of TYR/Au NPs/Ab_2 bioconjugates' solution for 60 min, and

again thoroughly washed. Afterwards, 10 μL of 5.0 mM tyrosine, 10 μL pH=7.0 HAc-NaAc buffer solution and 10 μL of 0.15 mg/mL TiO_2 was added for an incubation time of 10 min at 37 ºC. Finally, 20 μL of 100 mg/mL HRP, 130 μL of acetate buffer (pH=4.0) and 20 μL of 5.0 mM TMB were added into the above 96 well plates and illuminated for 15 min under visible light ($\lambda \geq 400$ nm) irradiation, and the absorbance of oxTMB at 652 nm was measured.

The APE-1 from real samples were also detected. Human serum samples from healthy volunteers were collected from Jiangnan University Hospital (WuXi, Jiangsu province). Thereafter, the mixture was centrifuged for 10 min at 10,000 rpm to remove insoluble materials and the supernatant was centrifuged once again. Finally, the extract diluted with the appropriate volume ($1:10^5$) was spiked with known quantities of APE-1 and was assayed by the procedure described above. The acceptable recoveries from 96.7% to 112.0% for APE-1 (shown in Table S2) in human serum sample analysis suggested feasibility of the method in practical detection. In addition, the APE-1 in two serum samples (diluted by 10-fold) from healthy adults were also detected by the commercially available enzyme-linked immunosorbent assay (ELISA) kit (LifeSpan BioSciences, USA) and the proposed method for comparision. For the detection of the two serum samples from healthy adults, the results of 1.30±0.04 and 1.68±0.05 ng/mL (for 10-fold diluted samples) by the commercially available enzyme-linked immunosorbent assay (ELISA) kit were in good agreement with that of 1.22±0.03 and 1.75±0.06 pg/ml (for 10^4-fold diluted samples) through the proposed method, indicating the acceptable accuracy of the developed method.

Live subject statement

All the experiments were performed in compliance with the relevant laws and institutional guidelines. The experiments involving human serums were approved by the Institutional Ethical Committee of Jiangnan University. This committee has informed consent from the volunteers who provided the serum samples for experimentation with human subjects.

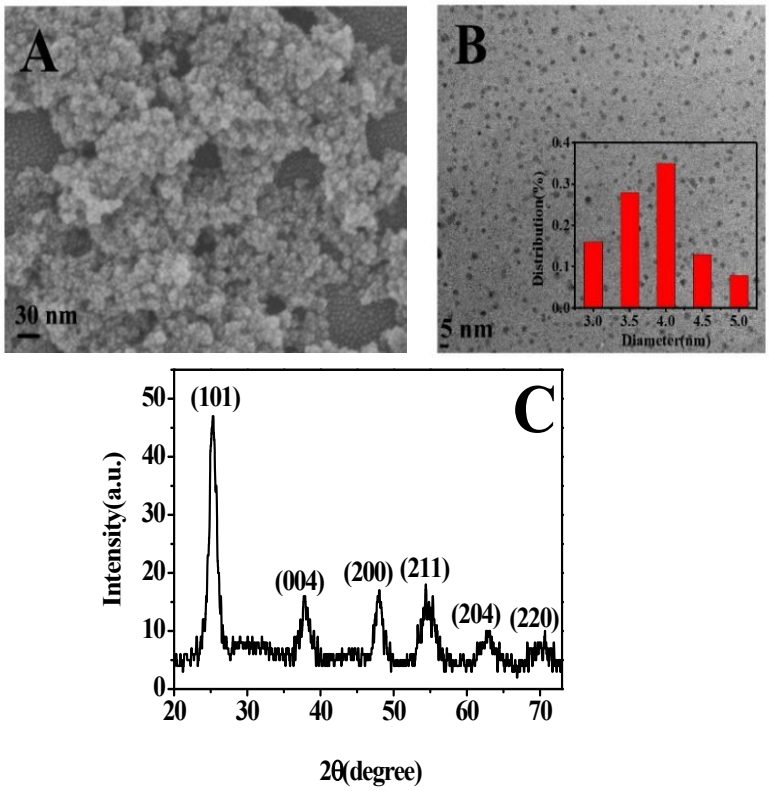

Fig.S1 SEM (A), TEM (B) images and XRD pattern (C) of the synthesized TiO_2 NPs. Inset image in B: size distribution of the synthesized TiO_2 NPs in diameter.

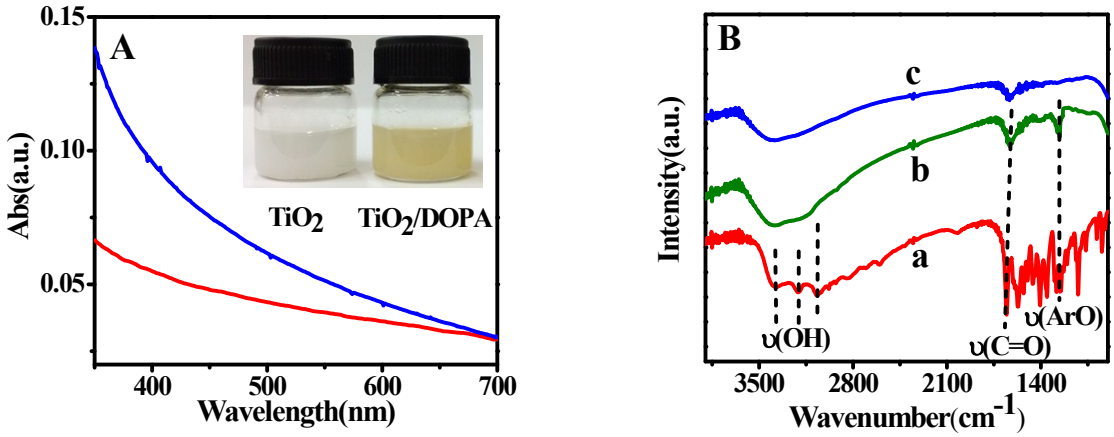

Fig.S2 (A) The varied absorption spectrum of TiO_2 NPs before (red line) and after (blue line) coordinating with DOPA and the corresponding color change (insert image). (B) The variation of the FT-IR spectra of DOPA after its coordination with TiO_2 NPs: (a) DOPA, (b) TiO_2/DOPA and (c) TiO_2 NPs.

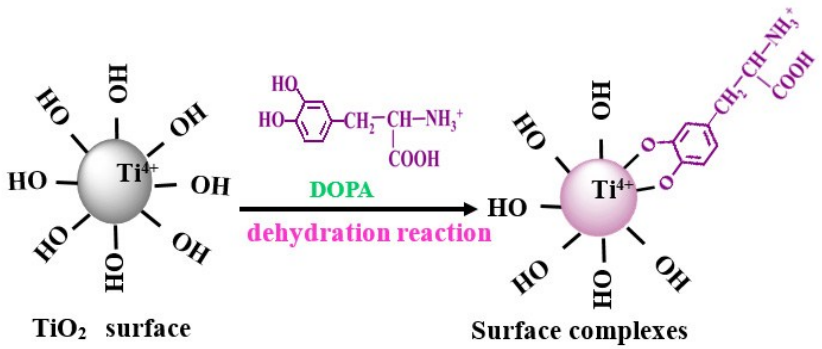

Fig.S3 Schematic illustration of the formation of TiO_2/DOPA through the coordination of DOPA on TiO_2 surface.

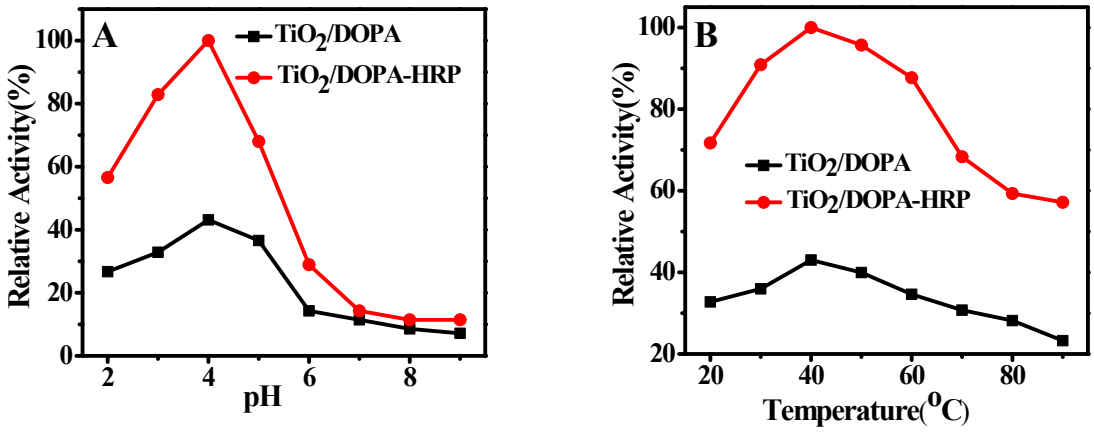

Fig.S4 The influence of buffer solution pH (A) and temperature (B) on the relative catalytic activity of the TiO_2/DOPA and the TiO_2/DOPA-HRP systems.

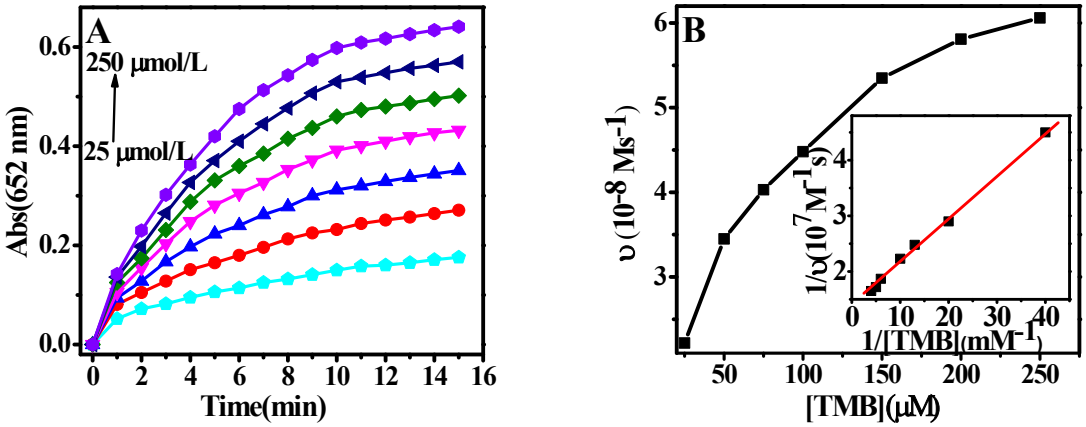

Fig.S5 (A) Performances of the catalytic system of TiO_2/DOPA-HRP in the presence of different concentrations of TMB (25, 50, 75, 100, 150, 200, 250 μmol/L) at different reaction times. (B) Steady-state kinetic assay of the TiO_2/DOPA-HRP system for TMB oxidation under visible light irradiation ($\lambda \geq 400$ nm). Insets are the Lineweaver-Burk plots of the double reciprocal of the Michaelis-Menten equation. Conditions: 0.01 mg/mL TiO_2/DOPA, acetate buffer pH=4.0, [HRP]=10 mg/L.

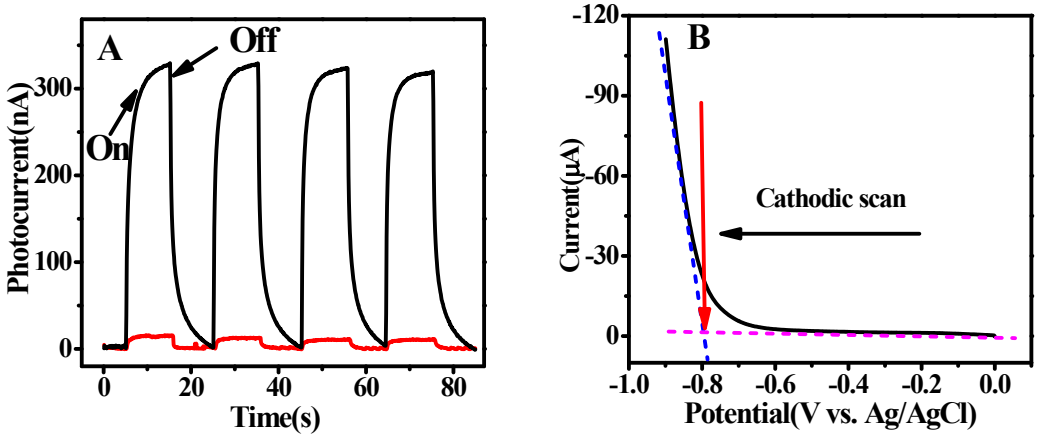

Fig.S6 (A) Photocurrent-time performances of TiO_2 (red line) and TiO_2/DOPA (black line) modified ITO electrode at an applied potential of 0 V (vs saturated Ag/AgCl) in 0.1 mol/L Na_2SO_4 aqueous solution under visible light irradiation ($\lambda \geq 400$ nm). (B) Cathodic linear potential scan for determining the conduction band edge of TiO_2/DOPA specimens at 5 mV/s.

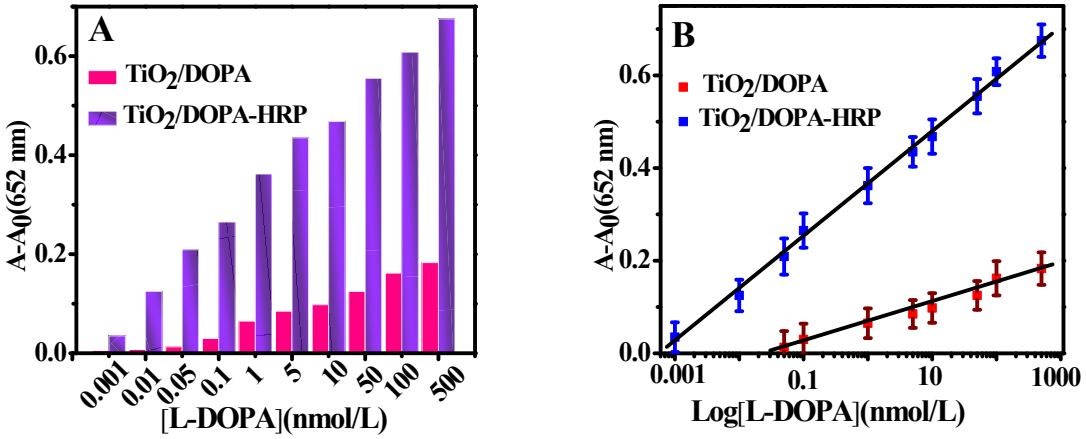

Fig.S7 (A) Comparison of the responses of the TiO_2/DOPA and TiO_2/DOPA-HRP systems to DOPA by the absorption changes of oxTMB, and (B) the corresponding linear calibration curves.

Table S1. Comparison of different assays for TYR detection

Method	Material	Detection limit (U/mL)	Linear range (U/mL)	Reference
Electrochemistry/Photo−electrochemistry	Pt or CdS NPs	1.0/0.10	Not given	3
Fluorescence	Au NCs	6.0×10^{-3}	6.0×10^{-3}–3.6	4
Fluorescence	DOPA-CQDs	7.0×10^{-3}	2.3×10^{-2}–0.8	5
Fluorescence	Au NCs	8.0×10^{-2}	$0.5\text{-}2.0\times10^{2}$	6
Fluorescence	Ag NCs	1.0×10^{-4}	Not given	7
Colorimetry	TiO_2 NPs and HRP	2.5×10^{-5}	1.0×10^{-4}-50	This work

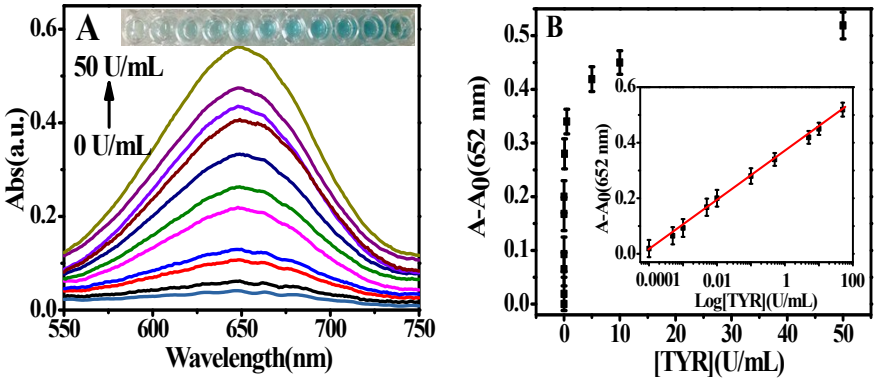

Fig.S8 (A) Colorimetric (insert image) and UV-Vis absorption spectroscopic detection of TYR through the biocatalytic cascade. (B) The linear calibration plots for TYR detection. Error bars represent the standard deviation of four repeated measurements.

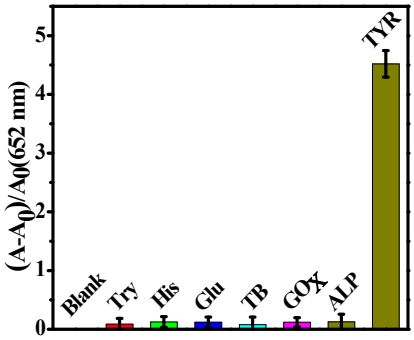

Fig.S9 Selectivity of the protocol for TYR (0.5 U/mL) by comparing the response with other interferents. The concentrations of alkaline phosphate (ALP), glucose oxidase (GOx), thrombin (TB) and trypsin (Try) are 5.0 U/mL, the concentrations of glucose (Glu) and histidine (His) is 0.01 mg/mL.

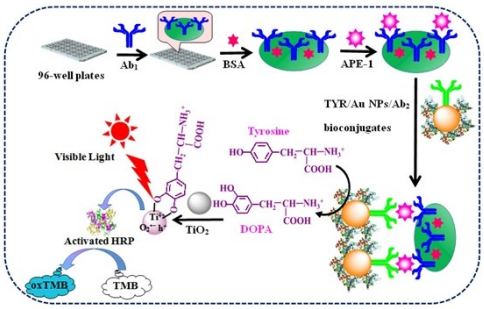

Scheme S1. Immunoassay for APE-1 based on the photoswitchable enzyme cascade.

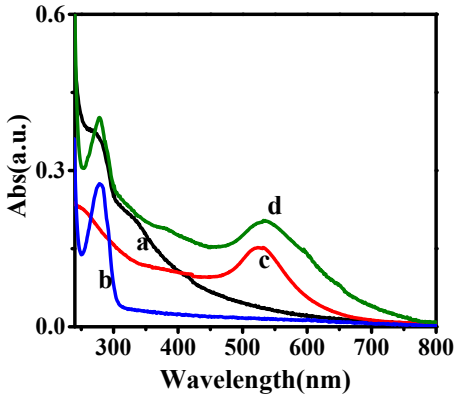

Fig.S10 (A) UV−vis absorption spectra of (a) TYR, (b) Ab_2, (c) Au NPs, and (d) TYR/Au NPs/Ab_2.

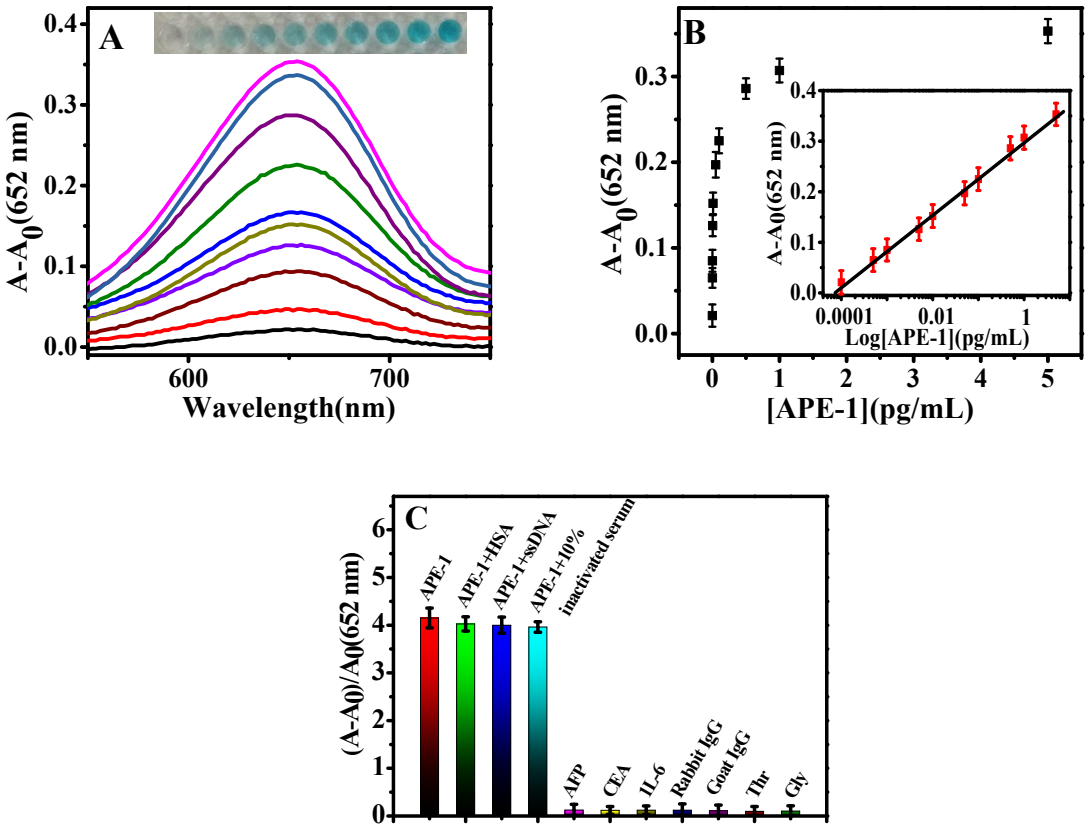

Fig.S11 (A) Colorimetric (insert image) and UV-Vis absorption spectroscopic detection of APE-1 through the biocatalytic cascade. (B) The linear calibration plots for APE-1 detection. Error bars represent the standard deviation of four repeated measurements. (C) Selectivity of the protocol for APE-1 (1.0 pg/mL) by comparing the response with other interferents. The concentrations of alpha fetoprotein (AFP), carcinoembryonic antigen (CEA), interleukin-6 (1L-6), rabbit IgG, and goat IgG are 10.0 pg/mL, the concentrations of glycine (Gly) and threonine (Thr) are 0.01 mg/mL. The responses from the mixture of 50 mg/mL human serum albumin (HSA) or 20 ng/mL of 20 mer single stranded DNA (ssDNA) with APE-1 (1.0 pg/mL), and APE-1 (1.0 pg/mL) in heat-inactivated serum (at 10-fold dilution) are also recorded.

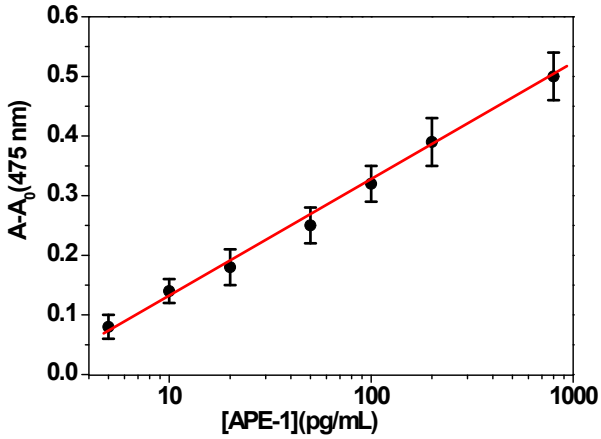

Fig.S12 Immunoassay of APE-1 using conventional TYR-based catalyzed oxidation of tyrosine to generate dopachrome (with characteristic absorption at 475 nm) as the signal reporter. The TYR/Au NPs/Ab_2 bioconjugates synthesized as reported in the experimental section was used as the label tracer.

Table S2. Determination of APE-1 in human serum sample by the proposed method

Real sample	APE-1 determined (pg/mL)	APE-1 spiked (pg/mL)	APE-1 detected (pg/mL)	Recovery %
Serum 1	0.13	0.15	0.29 ± 0.04	106.7
		0.30	0.42 ± 0.02	96.7
		0.50	0.69 ± 0.03	112.0

References

1 M. Addamo, V. Augugliaro, A. Di Paola, E. García-López, V. Loddo, Gi. Marcì, L. Palmisano, *Colloid. Surf. A: Physicochem. Eng. Aspects*, 2005, **265**, 23–31.

2 X. L. Hu, X. M. Wu, X. Fang, Z. J. Li, G. L. Wang, *Biosens. Bioelectron.*, 2016, **77**, 666–672.

3 H. B. Yildiz, R. Freeman, R. Gill, I. Willner, *Anal. Chem.*, 2008, **80**, 2811–2816.

4 Y. Teng, X. F. Jia, J. Li, E. K. Wang, *Anal. Chem.*, 2015, **87**, 4897−4902.

5 L. J. Chai, J. Zhou, H. Feng, C. Tang, Y. Y. Huang, Z. S. Qian, *ACS Appl. Mater. Interfaces*, 2015, **7**, 23564−23574.

6 X. M. Yang, Y. W. Luo, Y. Zhuo, Y. J. Feng, S. S. Zhu, *Anal. Chim. Acta*, 2014, **840**, 87–92.

7 X. Q. Liu, F. Wang, A. Niazov-Elkan, W. W. Guo, I. Willner, *Nano Lett.*, 2013, **13**, 309−314.